Bull Math Biol (2018) 80:1630–1654
https://doi.org/10.1007/s11538-018-0429-z

Society for Mathematical Biology

ORIGINAL ARTICLE

How Stochasticity Influences Leading Indicators of Critical Transitions

Suzanne M. O'Regan[1,2] · **Danielle L. Burton**[3]

Received: 1 December 2017 / Accepted: 29 March 2018 / Published online: 30 April 2018

Abstract Many complex systems exhibit critical transitions. Of considerable interest are bifurcations, small smooth changes in underlying drivers that produce abrupt shifts in system state. Before reaching the bifurcation point, the system gradually loses stability ('critical slowing down'). Signals of critical slowing down may be detected through measurement of summary statistics, but how extrinsic and intrinsic noises influence statistical patterns prior to a transition is unclear. Here, we consider a range of stochastic models that exhibit transcritical, saddle-node and pitchfork bifurcations. Noise was assumed to be either intrinsic or extrinsic. We derived expressions for the stationary variance, autocorrelation and power spectrum for all cases. Trends in summary statistics signaling the approach of each bifurcation depend on the form of noise. For example, models with intrinsic stochasticity may predict an increase in or a decline in variance as the bifurcation parameter changes, whereas models with extrinsic noise applied additively predict an increase in variance. The ability to classify trends of summary statistics for a broad class of models enhances our understanding of how critical slowing down manifests in complex systems approaching a transition.

Keywords Critical transitions · Bifurcations · Demographic stochasticity · Environmental stochasticity · Early warning signals · Additive noise · Multiplicative noise

✉ Suzanne M. O'Regan
smoregan@ncat.edu

1 Department of Mathematics, North Carolina A&T State University, Greensboro, NC 27411, USA

2 National Institute for Mathematical and Biological Synthesis, University of Tennessee, Knoxville, TN, USA

3 Department of Mathematics, University of Tennessee, Knoxville, TN 37996, USA

1 Introduction

Critical transitions are a feature of many complex natural systems, e.g., (Scheffer et al. 2009, 2012; Lenton 2011; Trefois et al. 2015; Quail et al. 2015). Examples of critical transitions in environmental systems include eutrophication of lakes (Scheffer et al. 1993), collapse of pollinator communities (Lever et al. 2014), shifts in atmospheric circulation (Lenton et al. 2008) and elimination of infectious diseases (Drake and Hay 2017). Bifurcations, small smooth changes in system parameters that induce sudden shifts in system behavior, are of considerable interest because they provide mechanistic models for critical transitions that are driven by gradual directional change in underlying drivers. A bifurcation of a system may be anticipated because prior to reaching the dynamical threshold, the system gradually loses stability ('critical slowing down' (Wissel 1984; Strogatz 1994; Nes and Scheffer 2007)). Signatures of critical slowing down may be detectable through measurement of temporal summary statistics, such as variance, lag-1 autocorrelation and power spectrum (Scheffer 2009; Dakos et al. 2012). Trends in summary statistics may indicate an impending bifurcation.

To anticipate tipping points in natural systems, typically dynamical models are developed to produce predictions for leading indicator statistics (Scheffer et al. 2009; Dakos et al. 2012; Dai et al. 2013; Carpenter and Brock 2006; Veraart et al. 2012; Bauch et al. 2016). A common approach for generating leading indicator predictions is to simulate a single stochastic model with a slowly changing forcing variable through a bifurcation point and compare indicator predictions from the model with those measured from data. This approach has been referred to as the use of "metric-based indicators" (Dakos et al. 2012), where the expected statistical patterns produced from a model are compared with patterns found in data, as opposed to fitting models of critical transitions to data [use of a "model-based indicator" approach (Dakos et al. 2012; Boettiger and Hastings 2012; Lade and Gross 2012)]. Theory for leading indicator patterns is often derived from simple one-dimensional stochastic models with additive noise structure, where noise effects are superimposed on to the deterministic growth rate of stochastic differential equation models (Gardiner 2004; Kuehn 2011; Ditlevsen and Johnsen 2010; Nicolis and Nicolis 2014) or on to the return rate to equilibrium in autoregressive models (Scheffer et al. 2009; Ives et al. 2003; Ives and Dakos 2012). However, this approach does not specify the mechanisms behind the stochastic variation. It only assumes that it is caused by external forces, making it a form of process noise or environmental stochasticity. Alternatively, noise can affect the system through external variations in the environment that affect a specific rate of the system or a model parameter. In this case, the noise is applied in a multiplicative fashion to the deterministic model equations, and in ecology, it is the standard approach for modeling environmental stochasticity. Moreover, noise can be intrinsic to the system (i.e., operate at the microscale). In ecology, this is referred to as demographic stochasticity, where random effects are due to the inherent randomness of events such as births, deaths, immigration and emigration. What is unclear, however, is how extrinsic and intrinsic noise influence statistical patterns in temporal data prior to a bifurcation. For example, non-monotonic and decreasing patterns in variance prior to bifurcations have been described before in some models [e.g., (O'Regan and Drake 2013; O'Regan et al. 2016; Kuehn 2011; Dakos et al. 2012)]. In particular, it is unclear

what role the form of stochasticity may play in the behavior of variability indicators, such as variance and power spectrum, prior to a critical transition.

Here, we consider a broad class of minimal, one-dimensional stochastic differential equation models representing supercritical transcritical, saddle-node and pitchfork bifurcations of natural systems. Each model represents collapse of a stable system state. For example, we consider models of population extinction that are driven by a gradually decreasing intrinsic population growth rate, which approaches zero over a long time scale. The models are minimal in the sense that mechanistic, stochastic normal-form bifurcation models are used to examine the effects of intrinsic and external environmental noise on statistical patterns of variability. To show how critical slowing down manifests in statistical patterns generated by the models, we derived expressions for the stationary variance, autocorrelation and power spectrum for all cases. To investigate the robustness of our predictions, we used models of infectious disease elimination and overharvesting as case studies. We show that trends in variability statistics prior to bifurcation depend on noise structure, and consequently, patterns in certain indicators may not be generic.

2 Methods

2.1 Model Derivations

To mathematically describe system collapse in the simplest way possible, we write down canonical models describing supercritical transcritical bifurcation, saddle-node bifurcation and pitchfork bifurcations, respectively. All models can be transformed to a normal form through an appropriate change of variables (Strogatz 1994),

$$\frac{\mathrm{d}x}{\mathrm{d}t} = f(x, r), \tag{1}$$

where x is the variable of interest and r is the bifurcation parameter. The critical point in each model is $r = 0$, where a bifurcation occurs.

Using this framework, we consider three modes of system collapse. A supercritical transcritical bifurcation, modeled using $f(x, r) = rx - x^2$, describes the situation where the extinction state and the positive steady state $x^* = r > 0$ meet and exchange stability at $r = 0$. For example, models representing elimination of infectious disease may be reduced to this form. A catastrophic collapse is often modeled using a supercritical saddle-node bifurcation, described by $f(x, r) = r - x^2$, where the positive supercritical state $x^s = \sqrt{r}$ collides with the negative unstable state $x^u = -\sqrt{r}$, and is annihilated at $r = 0$. Hysteretic processes in ecology, e.g., eutrophication of lakes (Carpenter et al. 1999) or collapse of insect populations (Ludwig et al. 1978), can be reduced to a saddle-node normal form. Finally, a pitchfork bifurcation, $f(x, r) = rx - x^3$, is a model of population collapse that occurs due to the meeting of two stable states, $x^s = \pm\sqrt{r}$, and becoming a single extinction state at $r = 0$. Switching between two simultaneously stable climatic regimes or atmospheric states may be modeled by a reduction to supercritical pitchfork bifurcation normal form (Nicolis and Nicolis 2014). Bifurcation diagrams for each model are shown in Fig. 1.

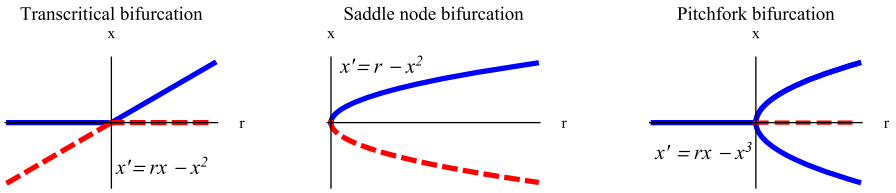

Fig. 1 Bifurcation diagrams for normal-form models (Color figure online)

To understand the effects of intrinsic and extrinsic variability on leading indicator patterns, we combine noise with the deterministic skeletons represented in Fig. 1 through development of three systems of stochastic differential equations for each bifurcation. Firstly, the effect of environmental variations is modeled through stochastic variation of the rate of change of the system variable, $f(x, r)$. The assumption of additive environmental noise on $f(x, r)$ is often used as the baseline model for studying the interplay between noise and behavior of a system approaching a bifurcation, particularly where it is not clear what the relative strengths of each noisy process that comprises $f(x, r)$ are. Secondly, we develop models with a mechanistic representation of environmental stochasticity, by assuming that the bifurcation parameter is a normally distributed random variable. Thirdly, we develop models that account for intrinsic microscale variations in the system variable (demographic stochasticity).

2.2 Form I: Additive Environmental Noise

To model the effect of extrinsic perturbations on each system, we assume the state variable $X(t)$ is a random variable and the system variable rate of change $f(X, r)$ is a noisy process due to extrinsic perturbations. The external perturbations are nonspecific in nature, in that they are assumed to not mechanistically affect any particular component of $f(X, r)$. More precisely, in a small increment of time Δt, the change in the system variable $\Delta X = X(t + \Delta t) - X(t)$ fluctuates randomly according to a normal distribution with mean $f(X, r)\Delta t$ and constant variance $\sigma^2 \Delta t$. We can write this assumption as an Itô stochastic differential equation, e.g., (Allen 2003),

$$\mathrm{d}X = f(X, r)\mathrm{d}t + \sigma \mathrm{d}W, \tag{2}$$

where $W(t)$ is a Wiener process with zero mean and variance Δt. Table 1 shows the models for each bifurcation, assuming additive environmental noise.

2.3 Form II: Mechanistic Environmental Noise

Alternatively, environmental noise may affect specific parameters of a system. In each of the bifurcation models we consider, we assume the bifurcation parameter r is influenced by environmental variations. In a small increment of time Δt, we assume

$$r\Delta t \sim \mathrm{Normal}(r\Delta t, \sigma^2 \Delta t), \tag{3}$$

Table 1 Mechanistic normal-form supercritical bifurcation population models written as Itô stochastic differential equations

Bifurcation	Form of stochasticity	Stochastic differential equation (SDE)
Transcritical bifurcation	Additive environmental noise	$\mathrm{d}X = (rX - X^2)\mathrm{d}t + \sigma \mathrm{d}W$
Transcritical bifurcation	Mechanistic environmental noise	$\mathrm{d}X = (rX - X^2)\mathrm{d}t + \sigma X \mathrm{d}W$
Transcritical bifurcation	Intrinsic noise	$\mathrm{d}X = (rX - X^2)\mathrm{d}t + \sqrt{rX + X^2}\mathrm{d}W$
Saddle-node bifurcation	Additive environmental noise	$\mathrm{d}X = (r - X^2)\mathrm{d}t + \sigma \mathrm{d}W$
Saddle-node bifurcation	Mechanistic environmental noise	$\mathrm{d}X = (r - X^2)\mathrm{d}t + \sigma \mathrm{d}W$
Saddle-node bifurcation	Intrinsic noise	$\mathrm{d}X = (r - X^2)\mathrm{d}t + \sqrt{r + X^2}\mathrm{d}W$
Pitchfork bifurcation	Additive environmental noise	$\mathrm{d}X = (rX - X^3)\mathrm{d}t + \sigma \mathrm{d}W$
Pitchfork bifurcation	Mechanistic environmental noise	$\mathrm{d}X = (rX - X^3)\mathrm{d}t + \sigma X \mathrm{d}W$
Pitchfork bifurcation	Intrinsic noise	$\mathrm{d}X = (rX - X^3)\mathrm{d}t + \sqrt{rX + X^3}\mathrm{d}W$

or $r\Delta t$ is normally distributed with mean $r\Delta t$ and variance $\sigma^2\Delta t$. Substituting in the normally distributed random variable $r\Delta t$ into the equation $\Delta X = f(X, r)\Delta t$ corresponding to each bifurcation and letting $\Delta t \to 0$, we obtain Itô stochastic differential equations in Table 1 that model mechanistic environmental noise. By assuming this form of mechanistic noise, the random perturbations scale with the state variable x in the models representing transcritical and pitchfork bifurcations, but they do not in the saddle-node bifurcation model (Table 1).

2.4 Form III: Intrinsic Noise

To model the effects of microscale noise, we derive stochastic differential equations from a Markov process. We consider two events: recruitment into the system, which increases the state variable X by a single unit in a small increment of time Δt, and removal from the system, which decreases the state variable by a single unit. Each event occurs according to a Poisson process and the transition probability of each event occurring in a short time period Δt is proportional to Δt. The probability of more than one event occurring during this time period is negligibly small (of order Δt). Table 2 shows the events and transition probabilities for each model. We apply a diffusion approximation to derive stochastic differential equations corresponding to the events in Table 2 (Allen 2003). Table 1 shows the stochastic differential equations representing intrinsic noise. Note that these events and rates are one choice representing intrinsic noise; alternative stochastic differential equations could be written depending on different underlying microscopic stochastic processes.

2.5 Obtaining Early Warning Signals

Each of the equations in Table 1 may be expressed in the general form

Table 2 Transition probabilities associated with changes in the state variable X

i	Transcritical bifurcation Transition probability p_i	Saddle-node bifurcation Transition probability p_i	Pitchfork bifurcation Transition probability p_i	$(\Delta X)_i$
1	$rX\Delta t$	$r\Delta t$	$rX\Delta t$	1
2	$X^2\Delta t$	$X^2\Delta t$	$X^3\Delta t$	-1
3	$1-(rX+X^2)\Delta t$	$1-(r+X^2)\Delta t$	$1-(rX+X^3)\Delta t$	0

$$\mathrm{d}X = f(X,r)\mathrm{d}t + \sqrt{g(X,r)^2}\mathrm{d}W. \tag{4}$$

The functions f and g^2, respectively, represent the drift and diffusion coefficients of the forward Kolmogorov equation associated with equation (4) (Allen 2007). To quantify the behavior of small perturbations from the positive supercritical equilibrium state, we linearize the drift and diffusion coefficients of the forward Kolmogorov equation around the supercritical steady state $x^s > 0$. Letting $\hat{X(t)} = X(t) - x^s$ represent deviations from the equilibrium and retaining leading order terms in the expansions, the stochastic differential equation for their evolution is an Ornstein–Uhlenbeck (O–U) process,

$$\mathrm{d}\hat{X} = f'(x^s,r)\hat{X}\mathrm{d}t + \sqrt{g(x^s,r)^2}\mathrm{d}W. \tag{5}$$

Consequently, the dynamics of perturbations from equilibrium are governed by Eq. (5). The linearized drift term is the eigenvalue of the corresponding deterministic model (1), and the magnitude of the linearized drift term $|f'(x^s,r)|$ is the asymptotic decay rate of a perturbation, known as engineering or asymptotic resilience in ecology (Pimm 1984; Holling 1996), or simply resilience. Depending on the nature of the system noise, the variance $g(x^s,r)^2$ of the O–U perturbation process (hereafter referred to as O–U variance) may depend on the steady state x^s, which is decreasing to zero in the supercritical models.

Standard approaches, e.g., (Gardiner 2004; Allen 2003; Nisbet and Gurney 1982), yield expressions for key summary statistics. The lag-τ autocorrelation function is

$$a(r) = \exp\left(-|f'(x^s,r)|\tau\right). \tag{6}$$

The lag-τ autocorrelation only depends on resilience $|f'(x^s,r)|$. In contrast, variance, coefficient of variation and power spectrum all depend on the O–U variance $g(x^s,r)^2$. The power spectrum of the fluctuations in terms of angular frequencies ω may be determined through Fourier transformation of Eq. (5),

$$S_r(\omega) = \frac{g(x^s,r)^2}{(|f'(x^s,r|))^2+\omega^2)}. \tag{7}$$

The stationary variance of the state variable

$$v(r) = \frac{g(x^s, r)^2}{2|f'(x^s, r)|}, \tag{8}$$

may be found by either Fourier transforming Eq. (5) [e.g., (Nisbet and Gurney 1982)] and through integrating the expression for the power spectrum, or directly by taking expectations [e.g., (Allen 2003)]. Finally, the coefficient of variation is the standard deviation $\sqrt{v(r)}$ normalized by the steady state, x^s,

$$cv(r) = \frac{\sqrt{v(r)}}{x^s}. \tag{9}$$

To examine how the summary statistics behave as the bifurcation point is approached, we derived analytical expressions for each statistic using each of the models in Table 1 and examined their behavior in the limit $r \to 0$ from the right.

3 Results

The expressions for variance, coefficient of variation and power spectrum differ for each form of stochasticity, as these statistics depend on the noise mechanism (Tables 3, 4, and 5). The autocorrelation function is the same for all stochasticity types, as it depends only on the magnitude of the return rate to equilibrium. Three limiting behavior outcomes for variance arise from the models of noise mechanism and bifurcation combinations (Table 6). Variance approaches positive infinity, zero or a nonzero constant. In all models, all variance quotients have a discontinuity at the bifurcation point, and the denominator in the variance quotient tends to zero as the bifurcation point is approached,

$$\lim_{r \to 0^+} 2|f'(x^s, r)| = 0. \tag{10}$$

For the models considered in Table 1, notice that the limit of the O–U variance in each model, $\lim_{r\to 0^+} g^2(x^s, r)$, is either σ^2 or zero (Tables 3, 4, and 5). If $\lim_{r\to 0^+} g^2(x^s, r) = \sigma^2$, then the variance quotient $v(r)$ will diverge. This outcome is predicted if environmental stochasticity is assumed to affect the system growth rate $f(X, r)$ as a whole (additive noise). For example, in the simplest stochastic model for a system approaching a critical transition, extrinsic noise is assumed to be additive, and O–U variance is assumed to be independent of the bifurcation parameter. In this model, the eigenvalue $f'(x^s, r)$ shrinks relative to O–U variance, which stays constant, and the stationary variance of the state variable $X(t)$ blows up as r approaches the bifurcation point.

A necessary condition for the variance of $X(t)$ to approach zero is that the limit of the O–U variance must approach zero. Canceling common factors in the variance quotient (8) yields limits of zero in normal-form models of bifurcations with demographic stochasticity, and in the transcritical bifurcation model with mechanistic environmental

Table 3 Summary stationary statistics derived from transcritical bifurcation normal-form SDEs (Table 1), assuming $r > 0$, $x^s = r$ is stable, and eigenvalue $f'(x^s, r) = -r$

Stochasticity type	O–U variance $g^2(x^s, r)$	Autocorrelation	Power spectrum	Variance of $X(t)$ $v(r)$	Coefficient of variation $cv(r)$
Additive environmental noise	σ^2	$\exp(-r\tau)$	$\frac{\sigma^2}{(r^2+\omega^2)}$	$\frac{\sigma^2}{2r}$	$\frac{\sigma}{\sqrt{2}r^{\frac{3}{2}}}$
Mechanistic environmental noise	$\sigma^2 r^2$	$\exp(-r\tau)$	$\frac{(\sigma r)^2}{(r^2+\omega^2)}$	$\frac{\sigma^2 r}{2}$	$\frac{\sigma}{\sqrt{2r}}$
Intrinsic noise	$2r^2$	$\exp(-r\tau)$	$\frac{2r^2}{(r^2+\omega^2)}$	r	$\frac{1}{\sqrt{r}}$

Table 4 Summary statistics derived from saddle-node bifurcation normal-form stochastic differential equations (Table 1), assuming $r > 0$, $x^s = \sqrt{r}$ is stable, and eigenvalue $f'(x^s, r) = -2\sqrt{r}$

Stochasticity type	O–U variance $g^2(x^s, r)$	Autocorrelation	Power spectrum	Variance of $X(t)$ $v(r)$	Coefficient of variation $cv(r)$
Additive environmental noise	σ^2	$\exp(-2\sqrt{r}\tau)$	$\frac{\sigma^2}{(4r+\omega^2)}$	$\frac{\sigma^2}{4\sqrt{r}}$	$\frac{\sigma}{2r^{\frac{3}{4}}}$
Mechanistic environmental noise	σ^2	$\exp(-2\sqrt{r}\tau)$	$\frac{\sigma^2}{(4r+\omega^2)}$	$\frac{\sigma^2}{4\sqrt{r}}$	$\frac{\sigma}{2r^{\frac{3}{4}}}$
Intrinsic noise	$2r$	$\exp(-2\sqrt{r}\tau)$	$\frac{2r}{(4r+\omega^2)}$	$\frac{\sqrt{r}}{2}$	$\frac{1}{\sqrt{2}r^{\frac{1}{4}}}$

Table 5 Summary statistics derived from pitchfork bifurcation normal-form stochastic differential equations (Table 1), assuming $r > 0$, $x^s = \sqrt{r}$ is stable, eigenvalue $f'(x^s, r) = -2r$

Stochasticity type	O–U variance $g^2(x^s, r)$	Autocorrelation	Power spectrum	Variance of $X(t)$ $v(r)$	Coefficient of variation $cv(r)$
Additive environmental noise	σ^2	$\exp(-2r\tau)$	$\frac{\sigma^2}{(4r^2+\omega^2)}$	$\frac{\sigma^2}{4r}$	$\frac{\sigma}{2r}$
Mechanistic environmental noise	$\sigma^2 r$	$\exp(-2r\tau)$	$\frac{\sigma^2 r}{(4r^2+\omega^2)}$	$\frac{\sigma^2}{4}$	$\frac{\sigma}{2\sqrt{r}}$
Intrinsic noise	$2r^{3/2}$	$\exp(-2r\tau)$	$\frac{2r\sqrt{r}}{(4r^2+\omega^2)}$	$\frac{\sqrt{r}}{2}$	$\frac{1}{\sqrt{2}r^{1/4}}$

Table 6 Limiting behavior of stationary variance $v(r)$ and coefficient of variation $cv(r)$ of state variable $X(t)$

Bifurcation	Stochasticity type	Variance limiting behavior ($\lim_{r\to 0^+} v(r)$)	CV limiting behavior ($\lim_{r\to 0^+} cv(r)$)
Transcritical	Additive environmental noise	$+\infty$	$+\infty$
Transcritical	Mechanistic environmental noise	0	$+\infty$
Transcritical	Intrinsic noise	0	$+\infty$
Saddle-node	Additive environmental noise	$+\infty$	$+\infty$
Saddle-node	Mechanistic environmental noise	$+\infty$	$+\infty$
Saddle-node	Intrinsic noise	0	$+\infty$
Pitchfork	Additive environmental noise	$+\infty$	$+\infty$
Pitchfork	Mechanistic environmental noise	$\sigma^2/4$	$+\infty$
Pitchfork	Intrinsic noise	0	$+\infty$

noise. In each model, $\lim_{r\to 0^+} g^2(x^s, r) = 0$. Additionally, O–U variance declines to zero more rapidly than resilience in a neighborhood of the bifurcation point [Fig. 2a–c, compare blue dashed lines, representing O–U variance due to intrinsic noise, to thick black line (resilience)]. Notice that in these cases, simplification is not needed to evaluate the limit of the variance quotient; rather, L'Hospital's rule may be used, since the numerator and denominator both approach zero, yielding an indeterminate form. When L'Hospital's rule is applied to evaluate the variance limits in these models, the limit of the derivatives of the numerator and the denominator is zero. The exceptional case is the pitchfork bifurcation model with mechanistic environmental noise, where it is easy to see that L'Hospital's rule yields a nonzero limit. Although $\lim_{r\to 0^+} g^2(x^s, r) = 0$ in this model, simplification of the variance expression yields constant variance of $\sigma^2/4$ as r approaches zero from the right. This occurs because O–U variance and resilience both scale with r (Fig. 2c). Taken together, these observations suggest that that there are two key ingredients required for variance of one-dimensional stochastic supercritical bifurcation systems to approach zero: on approaching the bifurcation point, the limit of O–U variance must approach zero, and O–U variance must vanish more rapidly than resilience. We establish this statement formally in "Appendix A."

The argument in "Appendix A" can be generalized to the coefficient of variation, $cv(r)$, by replacing $v(r)$ with $cv(r)$, $g(x^s, r)^2$ with $v(r)$ and $2|f'(x^s, r)|$ with x^s. The coefficient of variation will blow up near criticality when the magnitude of the steady state becomes less than the standard deviation of the perturbation process (i.e., the steady state approaches zero from the right faster than the standard deviation). This is true as each bifurcation is approached under all noise regimes, because the standard deviation also depends on the steady state.

The power spectrum depends on the variance of the Ornstein–Uhlenbeck perturbation process (Tables 3, 4 and 5). As r approaches zero from the right, the graph of the power spectrum stretches vertically, and consequently, lower angular frequencies ω dominate the spectrum. Comparing across noise types, the power spectrum changes in the vertical direction (i.e., strength of the signal). Although all power spectra have the

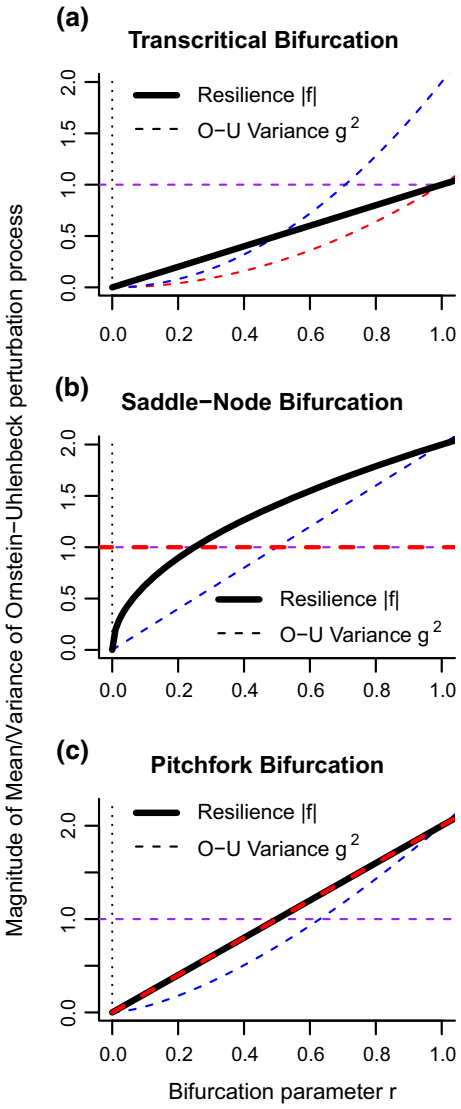

Fig. 2 Magnitude of the mean (resilience $|f'(x^s, r)|$) and variance $g^2(x^s, r)$ of the Ornstein–Uhlenbeck perturbation process for each normal-form bifurcation model. The terms comprise the denominator and numerator of the state variable stationary variance quotient (8), respectively. Bold lines show resilience as a function of the bifurcation parameter r. Dashed lines describe O–U variance as a function of r (purple dashed lines: additive environmental noise, $\sigma^2 = 1$; blue dashed lines: intrinsic noise; red dashed lines: mechanistic environmental noise). As the critical threshold $r^* = 0$ (dotted vertical line) is approached from the right, either resilience dominates O–U variance in the variance quotient $v(r)$ (i.e., resilience graph lies above O–U variance graph), or the O–U variance dominates the effect of the resilience on the variance quotient (O–U variance graph lies above resilience). Resilience and O–U variance functions for each model are listed in Tables 3, 4 and 5 (Color figure online)

same functional form with respect to angular frequency ω, the vertical scaling factors differ and so the normalized area under the curve (stationary variance or fluctuation intensity) is different for each noise form. In general, less power will be observed in the signal (i.e., fluctuation intensity will be weaker) if O–U variance depends on the bifurcation parameter (e.g., compare power spectra expressions derived from bifurcation models with intrinsic stochasticity with those from additive environmental noise in Tables 3, 4 and 5).

Clearly, the behavior of the variance of the Ornstein–Uhlenbeck perturbation process (5) close to the critical point influences the behavior of the statistics prior to the

bifurcation and subsequent detection of critical slowing down. This observation has been made before in the context of ecological models for overharvesting (Dakos et al. 2012) but not in the context of generic models for critical transitions. Moreover, here we establish a mechanism for state variable variance blow-up vs. variance decay: how the relative magnitudes of the noise component and the deterministic component of the Ornstein–Uhlenbeck perturbation process change with respect to the bifurcation parameter. In sum, if resilience declines to zero more quickly than O–U variance, noise will dominate dynamics prior to bifurcation, and state variable variance will diverge, whereas if O–U variance declines to zero more quickly (e.g., if it scales with system size), then the deterministic return to equilibrium will dominate dynamics and variance will approach zero.

It is crucial to note that the long-term behavior of the statistics prior to the critical transition depends on the mechanistic assumptions we have made to derive normal-form stochastic models. Normal-form models are generic, and it is possible, under suitable transformations, to write any one-dimensional model in the appropriate normal form (Strogatz 1994). However, transforming a model into normal form is a specialized mathematical technique (Guckenheimer and Holmes 1983), which becomes difficult when the system under consideration is multidimensional. To test the robustness of the theory, we relax the use of the minimal normal-form model framework. Next, we use mechanistic epidemiological and ecological models approaching critical transitions as case studies.

4 Testing the Theory: SIS Model as a Case Study

In Sect. 3 we observed that trends in variance prior to critical transitions are especially affected by noise mechanism. To investigate the robustness of the predictions for variance obtained from the mechanistic normal-form models, we derived statistics for a suite of stochastic epidemiological models approaching elimination (a supercritical transcritical bifurcation) under multiple sources of noise, without transforming the models to a normal form. Specifically, we examined variance predictions obtained from mechanistic, stochastic susceptible–infectious–susceptible (SIS) models. Emergence of zoonotic diseases (Karesh et al. 2012; Han and Drake 2016), and global eradication of smallpox (Drake and Hay 2017) are examples of critical transitions in epidemiology. Indicators of critical slowing down may be useful for obtaining a measure of how close a disease system is to elimination (Drake and Hay 2017).

Assuming a well-mixed population that is closed and has population size N and infectious individuals become susceptible on recovery, the deterministic SIS model is

$$\begin{aligned} \frac{\mathrm{d}S}{\mathrm{d}t} &= \gamma I - \frac{\beta SI}{N} \\ \frac{\mathrm{d}I}{\mathrm{d}t} &= \frac{\beta SI}{N} - \gamma I. \end{aligned} \tag{11}$$

As the population size is constant and $S = N - I$, model (11) is equivalent to a single equation for the rate of change of infectious individuals only,

$$\frac{\mathrm{d}I}{\mathrm{d}t} = \frac{\beta(N-I)I}{N} - \gamma I,$$

which can be written as,

$$\frac{\mathrm{d}I}{\mathrm{d}t} = (\beta - \gamma)I - \frac{\beta I^2}{N}. \tag{12}$$

Equation (12) has two steady states: the endemic equilibrium $I^* = N(1 - \gamma/\beta)$ and the disease-free equilibrium $I_0 = 0$. The basic reproduction number for model (11) is $R_0 = \beta/\gamma$. The SIS model has a transcritical bifurcation point at $R_0 = 1$, where the endemic equilibrium and the disease-free equilibrium meet and exchange stability. At $R_0 = 1$, the transmission rate equals the recovery rate, $\beta^* = \gamma^*$. Equation (12) can be expressed in the normal form for a transcritical bifurcation, by using the transformation $x = \frac{\beta I}{N}$ and setting $r = \beta - \gamma$.

A supercritical SIS model, where $R_0 > 1$ is gradually decreasing to the critical threshold at unity, is representative of an SIS epidemic system forced through elimination due to changes in epidemiological processes (model parameters) that occur over long time scales. For example, reduction in the per-capita transmission rate can result from reduction in contact with other individuals through the use of protective measures such as wearing masks or using antibacterial agents. Reduction in transmission rate reduces R_0. On the other hand, R_0 may be reduced by increases in per-capita recovery rate, e.g., through shortening of the infectious period of the disease resulting from provision of drugs or other therapeutic treatments that quicken recovery.

4.1 Stochastic Models

Models (a), (b) and (c) in Table 7 assume SIS processes that are driven by environmental stochasticity (e.g., variation in environmental conditions such as temperature, humidity etc.) In these models, the effects of environmental stochasticity on per-capita transmission and recovery rates, respectively, dominate any effects of variation arising from infection and recovery events. Model (a) assumes the growth rate of infectious individuals fluctuates randomly due to normally distributed environmental drivers. Model (b) assumes that the per-capita transmission rate β fluctuates randomly due to external environmental forces, whereas model (c) assumes that the per-capita recovery rate γ experiences noisy perturbations from the external environment. Model (a) is an additive noise model, and model (c) bears a close resemblance to the normal-form model approaching a transcritical bifurcation subject to a mechanistic noise regime (Table 1). Model (c) can also represent an SIS system exhibiting fluctuations in intrinsic growth rate $r = \beta - \gamma$, which are driven by variability in recovery rate.

Additionally, we derived two models driven by demographic stochasticity (models (d) and (e) in Table 7). Events are infection (transmission of the infection from infectious to susceptible individuals) and recovery of infectious individuals. Each event

Table 7 Stochastic SIS models

Model	Stochasticity type	Equations
(a)	Additive environmental noise	$\mathrm{d}I = \left(\frac{\beta(N-I)I}{N} - \gamma I\right)\mathrm{d}t + \sigma \mathrm{d}W_1$
(b)	Mechanistic environmental noise (i)	$\mathrm{d}I = \left(\frac{\beta(N-I)I}{N} - \gamma I\right)\mathrm{d}t + \sigma \frac{(N-I)I}{N}\mathrm{d}W_2$
(c)	Mechanistic environmental noise (ii)	$\mathrm{d}I = \left(\frac{\beta(N-I)I}{N} - \gamma I\right)\mathrm{d}t + \sigma I \mathrm{d}W_3$
(d)	Mechanistic demographic noise (i)	$\mathrm{d}I = \left(\beta\frac{(N-I)I}{N} - \gamma I\right)\mathrm{d}t + \sqrt{\frac{\beta(N-I)I}{N} + \gamma I}\mathrm{d}W_4$
(e)	Mechanistic demographic noise (ii)	$\mathrm{d}I = \left((\beta-\gamma)I - \frac{\beta I^2}{N}\right)\Delta t + \sqrt{(\beta-\gamma)I + \frac{\beta I^2}{N}}\mathrm{d}W_5$

Table 8 SIS stochastic processes

Event i	ΔI_i	Model (d) p_i	Model (e) p_i
Infection	$+1$	$\frac{\beta(N-I)I}{N}\Delta t$	$(\beta-\gamma)I\Delta t$
Recovery	-1	$\gamma I \Delta t$	$\frac{\beta I^2}{N}\Delta t$

occurs according to a Poisson process and the transition probability of each event occurring in a short time period Δt is proportional to Δt. Changes in the infectious population are denoted by $\Delta I = I(t+\Delta t) - I(t)$. Table 8 shows the events and transition probabilities p_i for the two processes; notice that the transition probabilities for processes (d) and (e) differ. Model (d) is a realistic representation of an SIS epidemiological process, whereas model (e) represents the epidemiological process as a logistic growth process, and was developed to have a similar structure to the normal-form model of a transcritical bifurcation under demographic noise in Table 1. Using a diffusion approximation leads to stochastic differential equations for these processes (Allen 2003). The stochastic processes governing changes in infectious individuals (d) and (e) have the same mean but the variance for the two processes differ.

4.2 Stationary Variance Predictions as $R_0 \to 1$

Even for simple one-dimensional models, various limiting behaviors for the stationary variance of the infectious population are possible, depending on the mechanisms behind the stochastic SIS process (Table 9). The expressions for stationary variance depend on the underlying form of stochasticity and the interplay between O–U variance and system resilience. Linearizing the models in Table 7 yields the magnitude of the mean of the Ornstein–Uhlenbeck process; the resilience for models (a)–(e) is $|-(\beta-\gamma)|$, and therefore, the lag-τ autocorrelation function is $\exp(-|-(\beta-\gamma)|\tau)$. Resilience appears in the numerator of the variance quotient, rather than the denominator, under mechanistic environmental noise models (b) and (c). Consequently, variance approaches zero as R_0 approaches unity. Stationary variance equals the mean of the

Table 9 Behavior of stationary variance as $R_0 \to 1$

Model	O–U variance g^2	Variance	Limiting behavior ($R_0 \to 1$)	Trend (as $\beta \to \gamma^*$ from right)	Trend (as $\gamma \to \beta^*$ from left)
(a)	σ^2	$\frac{\sigma^2}{2(\beta-\gamma)}$	$+\infty$	Monotonic increase	Monotonic increase
(b)	$\frac{(\sigma I^*\gamma)^2}{\beta^2}$	$\frac{(\sigma N\gamma)^2(\beta-\gamma)}{2\beta^4}$	0	Non-monotonic in β	Non-monotonic in γ
(c)	$(\sigma I^*)^2$	$\frac{(\sigma N)^2(\beta-\gamma)}{2\beta^2}$	0	Non-monotonic in β	Monotonic decrease
(d)	$2(\beta-\gamma)(N-I^*)$	$\frac{N\gamma}{\beta}$	N	Monotonic increase	Monotonic increase
(e)	$2(\beta-\gamma)I^*$	$N\left(1-\frac{\gamma}{\beta}\right)$	0	Monotonic decrease	Monotonic decrease

Note that $I^* = N(1-\frac{\gamma}{\beta})$, and $\beta - \gamma > 0$. Note that for models (b), (d) and (e), we have fully simplified the O–U variance terms $g^2 = (\sigma(N-I^*)I^*/N)^2$, $g^2 = \beta(N-I^*)I^*/N + \gamma I^*$ and $g^2 = (\beta-\gamma)I^* + \beta(I^*)^2/N$

demographic SIS stochastic process (e), and thus, variance declines to zero as the critical threshold is approached. Alternatively, an increase in variance is observed under the more realistic demographic noise regime (d).

The opposing patterns in stationary variance can also be explained by the behavior of the equilibrium susceptible and infectious populations. Notice that for models (b), (c) and (e), O–U variance is positively correlated with the equilibrium or quasi-stationary mean of the infectious population, I^*, and thus, the variance of the perturbation process declines with the mean I^*. Stationary variance of the infectious population eventually declines to zero. On the other hand, in model (d), O–U variance is positively correlated with the equilibrium or quasi-stationary mean of the susceptible population, $N - I^*$, rather than the infectious population, and therefore the variance of the perturbation process increases with the increasing susceptible population as elimination of infectious individuals becomes more imminent. Consequently, the stationary variance increases.

Moreover, in some cases, stationary variance is a non-monotonic function of the bifurcation parameter. This prediction is in contrast to the monotonic (in intrinsic growth rate r) variance predictions for transcritical bifurcations under different noise types, in Table 3. For example, variance is non-monotonic with respect to β for model (b) in Table 7. To see this, we calculate the first derivative of the variance $v(\beta)$ with respect to β,

$$\frac{\mathrm{d}v(\beta)}{\mathrm{d}\beta} = \frac{(\sigma N\gamma)^2}{4\beta^4}\left(\frac{4\gamma}{\beta} - 3\right) \tag{13}$$

Setting expression (13) to zero and solving for β yields a single critical point at $\beta = 4\gamma/3$. The first derivative test shows the variance is monotonically increasing to the left as β approaches γ and is decreasing to the right. The variance declines as β decreases to γ (as R_0 approaches 1). Model (b) variance $v(\gamma)$ is also non-monotonic with respect to the bifurcation parameter γ (Table 9). Solving the expression $\frac{\mathrm{d}v(\gamma)}{d\gamma} = 0$ yields a single relevant critical point at $\gamma = 2\beta/3$. (The critical point at $\gamma = 0$ is not relevant for this model.) Variance increases to the left of the critical point and decreases to the right, and consequently, the variance decreases as R_0 tends to unity. Moreover, variance is a unimodal function of β, with a peak occurring at $\beta = 2\gamma$, assuming β is the bifurcation parameter in model (c). The variance decreases to the left of 2γ as β decreases to the bifurcation point at $\beta = \gamma$. Clearly, trends in variance prior to the bifurcation depend strongly on the underlying model structure.

To test the predicted relationships in Table 9 as a bifurcation parameter approaches the critical threshold, we conducted a simulation study. We examined trends in variance prior to the bifurcation point at $R_0 = 1$ as transmission rate β was decreased from 2 to 1.05 in increments of 0.05. For each value of the bifurcation parameter, we simulated each of the models over 1000 time steps, and calculated the stationary variance over the time series. The mean of the stationary variance, for each bifurcation parameter value, was obtained from 1000 simulations. All simulations were run using the package 'sde' in R v.3.3.1 and were initialized at the deterministic steady state corresponding to each value of transmission rate. Figure 3 compares the theoretical predictions for the

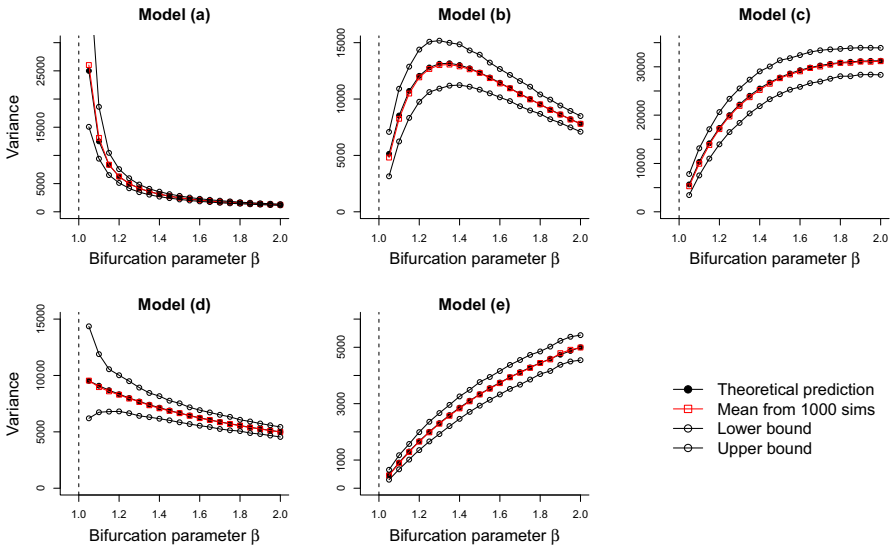

Fig. 3 Type of stochasticity affects trends in variance as transcritical bifurcations in stochastic SIS systems are approached. The dashed vertical line represents the critical threshold at $R_0 = 1$. Closed black circles represent theoretical predictions (Table 9), whereas open red squares represent the mean of the variance obtained from 1000 simulations of each model in Table 7. Black open circles represent 95% prediction intervals for variance calculated from simulations. Peaks in variance occur at $\beta = 4\gamma/3 = 4/3$ in **b** and at $\beta = 2\gamma = 2$ in **c**. Parameter values for simulations: $N = 10{,}000$, $\gamma = 1$, $\sigma = 50$ [additive noise model (**a**)], $\sigma = 0.05$ [mechanistic environmental noise models (**b**) and (**c**)] (Color figure online)

variance with variance predictions obtained from 1000 simulations of each model. As predicted by the theory in Table 9, variance increases as transmission rate β decreases in simulations of models (a) and (d), whereas realizations of models (b), (c) and (e) have decreasing variance as the critical threshold at $R_0 = 1$ (vertical line in each figure) is approached. Therefore, the predicted relationships with the bifurcation parameter of each model and the predicted limiting behavior are robust.

5 Testing the Theory: Saddle-Node Bifurcation Model with Decreasing Variance

Our analysis so far indicates that decreasing variance may be expected (and most likely) in systems where the bifurcation point is located at zero. Here we highlight a theoretical example where decreasing variance is the outcome prior to a saddle-node bifurcation that occurs at a nonzero bifurcation point.

Consider the following simple model for a logistically growing population subject to harvesting at constant rate h,

$$\frac{\mathrm{d}x}{\mathrm{d}t} = ax(1-x) - h. \tag{14}$$

Equation (14) has two steady states (Meiss 2007), which collide and disappear in a saddle-node bifurcation at $x^* = 1/2$. The harvest rate h is the bifurcation parameter, and the saddle-node bifurcation point occurs at $h^* = a/4$. In this model, population collapse is caused by increasing harvest rate h to the critical threshold h^*.

A decreasing trend in variance to zero may seem counterintuitive prior to population collapse through overharvesting, since the critical population level x^* is located at a nonzero value. Here we show that a declining variance pattern is at least theoretically possible. Consider the analogous stochastic differential equation for a population $X(t)$,

$$\mathrm{d}X = (aX(1-X) - h)\,\mathrm{d}t + \sqrt{\frac{a}{2} - aX(1-X) - h}\,\mathrm{d}W. \tag{15}$$

Equation (15) can be written in normal form, using the transformation (Meiss 2007),

$$\tau = at, \quad x = X - \frac{1}{2}, \quad r = \frac{1}{4} - \frac{h}{a}.$$

This transformation yields the supercritical saddle-node bifurcation model driven by demographic stochasticity (Table 1). Using Eq. (8) to obtain the variance $v(h)$ of the fluctuations of model (15) yields the expression,

$$v(h) = \frac{\frac{1}{2}(a - 4h)}{2\sqrt{a(a-4h)}}, \tag{16}$$

which is a decreasing function of h. It is easy to show using L'Hospital's rule that expression (16) approaches zero as $h \to h^*$ from the left.

An alternative stochastic model with same mean change in population size but different standard deviation is

$$\mathrm{d}X = (aX(1-X) - h)\,\mathrm{d}t + \sigma X(1-X)\,\mathrm{d}W. \tag{17}$$

This model assumes that the intrinsic growth rate, $a\Delta t$, is driven by environmental stochasticity, specifically, it is normally distributed with mean $a\Delta t$ and variance $\sigma^2\Delta t$. The expression for variance of the fluctuations is

$$v(h) = \frac{\sigma^2 h}{2a\sqrt{a(a-4h)}}. \tag{18}$$

Notice that the numerator increases and approaches $\sigma^2 h^*$, whereas the denominator approaches zero, and thus, expression (18) for variance blows up as $h \to h^*$ from the left. This example is consistent with the idea that saddle-node bifurcations are usually preceded by increasing variance.

6 Discussion and Conclusions

Critical slowing down is a generic phenomenon of systems approaching a bifurcation because the magnitude of the real part of the dominant eigenvalue approaches zero. Therefore, it is often assumed that patterns in leading indicators are also generic, because they should depend on the dominant eigenvalue. Until now, how extrinsic and intrinsic sources of noise interact with the deterministic dynamics of critical slowing down, manifested via system resilience, has been unclear. Our study aimed to elucidate how extrinsic and intrinsic noise (environmental and demographic stochasticity) affect leading indicators of critical transitions. We derived summary statistics for a broad class of bifurcations, under three noise regimes: additive noise, mechanistic environmental noise and intrinsic noise. Prior to a critical transition, trends in summary statistics of variability, such as variance and power spectrum, are sensitive to the underlying noise structure. In particular, variance may exhibit a wide range of limiting behavior prior to a critical transition, due to the interplay between system resilience and O–U variance of perturbations. Nonetheless, increasing trends in autocorrelation and coefficient of variation, together with shift of the power spectrum to lower frequencies, are patterns that are robust for all forms of stochasticity considered here.

Variance is usually expected to increase prior to a critical transition (Scheffer et al. 2009; Carpenter and Brock 2006; Ditlevsen and Johnsen 2010), but this expectation assumes that the system may be adequately represented by a model with additive noise. Use of this simple model, ubiquitous in the critical transitions literature, has promoted the expectation that variance will be amplified before a tipping point. Considering alternative noise mechanisms can result in different predictions for variance patterns, such as decreasing variance, or even no change in variance, e.g., prior to a pitchfork bifurcation in a multiplicative environmental noise regime. We have shown that variance patterns are due to the interaction between the deterministic component and the noise component of the perturbation decay process. Amplification of stochastic perturbations results from the perturbation process being dominated by its variance as its mean (resilience) shrinks to zero, and the stochastic process resembles a random walk. On the other hand, decreasing variance results from the variance of the perturbation decay process shrinking to zero and consequently, the perturbation process becomes dominated by the deterministic dynamics. Which of these patterns are more common in nature is unknown, but potentially, either of these patterns is possible. For example, decreasing variance might be expected in childhood immunizing disease systems (Keeling and Grenfell 1999), where the mean and the variance of the infectious population are correlated (O'Regan and Drake 2013; Keeling and Rohani 2008) or in ecological systems where the mean scales with variance according to a power-law relationship (Keeling 2000).

Dakos et al. (2012) used an overharvesting model with various forms of environmental noise to show that variance may increase or decrease prior to population collapse. The outcome depended on how environmental noise occurred in model parameters. For their particular models, variance declined but subsequently increased in the vicinity of the critical point. We expanded their results by considering a suite of models representative of the three supercritical bifurcations that can occur in one-dimensional

systems and by considering models with demographic noise. We show that the mechanisms behind the stochastic processes in the system determine the limiting behavior of variance prior to bifurcation.

The SIS models with demographic stochasticity explored in this paper [models (d) and (e) in Table 7] exhibit opposite trends in variance prior to elimination of disease. These models have the same mean return rate (resilience) but have different O–U variance, as a consequence of disparate assumptions about the nature of the processes driving dynamics. The O–U variance in model (d) is correlated with equilibrium number of susceptibles, resulting in increasing variance of the infectious population, since the number of susceptibles increases as the bifurcation point at $R_0 = 1$ is approached. The O–U variance in model (e) is correlated with equilibrium number of infectious individuals, which are declining to extinction, and hence variance of $I(t)$ declines in tandem with the number of infectious individuals. Similarly, the stochastic overharvesting models driven by two forms of stochasticity predicted opposing patterns in variance. Our analysis suggests that opposing patterns in indicators could be obtained from models of other systems approaching critical transitions that have the same deterministic representation, but invoke alternative representations of stochasticity. This makes it crucial to explore alternative mechanistic models for the system at hand.

We used the normal-form representation to develop minimal models for critical transitions. These models are minimal for the deterministic dynamics, but noise can be represented in multiple ways. It is important to point out that these models do not encompass all possible noise mechanisms; rather, the models represent thought experiments to explore some of the possibilities that could arise in reality. For example, the normal-form transcritical bifurcation model with intrinsic noise is not representative of all SIS models with demographic stochasticity [e.g., model (d) predicts increasing variance prior to bifurcation, rather than decreasing variance, which is predicted by the more general normal-form model]. What is clear is that different assumptions about noise mechanisms result in different predictions for variance trends.

We restricted our analysis to one-dimensional systems. We expect that the interaction between stochasticity and critical slowing down will be more complex in higher-dimensional systems, where statistics are likely to be nonlinear functions of multiple eigenvalues and the form of noise [e.g., (O'Regan and Drake 2013; Boerlijst et al. 2013)]. Our analysis additionally did not account for interactions between intrinsic and environmental stochasticity, or other sources of noise [e.g., correlated environmental noise (Sharma et al. 2014), measurement error (Ives et al. 2003), or demographic heterogeneity in ecological systems (Melbourne and Hastings 2008)]. To classify trends and limiting behavior of the leading indicators, we evaluated them about the steady state. We chose to simplify the analysis by not investigating trends in summary statistics obtained from stochastic fast-slow models because by Fenichel's theorem (Fenichel 1979), the dynamics of fast–slow models will approach those of the models where the bifurcation parameter is constant in the limit of the slow parameter approaching zero. Consequently, our results will hold when the bifurcation parameter changes over a long time scale. Moreover, we did not write our stochastic normal-form models formally [e.g., (Arnold 1998)], which usually leads to the noise appearing multiplicatively in the stochastic normal-form models (Nicolis and Nicolis 2014). Our development of stochastic normal-form models was inspired by the work of Boettiger

and Hastings (2012), who first described the detection of early warning signals based on critical slowing down as a model selection problem, and the approach of Kuehn (2011), which developed a multi-scale theory for critical transitions. Our approach compares multiple routes in which noise can affect dynamics to investigate how different noise representations affect trends in leading indicators of bifurcations.

The model analysis in this paper relies upon linearization of the stochastic differential equations about the steady state, which yields an Ornstein–Uhlenbeck process. If alternative attractors are present, perturbations from the steady state may grow large in the vicinity of the bifurcation point, e.g., via flickering between basins of attraction of alternative stable states (Dakos et al. 2013), and consequently, the error of the linear approximation of the true state of the system will grow. This could be particularly problematic if the transition is due to a saddle-node bifurcation, where stochastic switching between attractors is a common phenomenon (Wang et al. 2012). On the other hand, if the bifurcation point has been crossed, solutions may remain in the vicinity of the old or 'ghost' attractor, and potentially, the error obtained through the use of a first-order approximation could affect predictions for trends in leading indicators. More research is needed to establish how the error through the use of a linear approximation, rather than higher order approximations, affects leading indicator patterns in the neighborhood of the critical point, and to quantify sensitivity of leading indicators to this truncation error.

We assume that stochastic differential equations are an appropriate model for systems on the verge of transition because they provide a flexible framework for modeling a range of critical transitions and noise regimes, and analytical expressions for early warning signs are additionally straightforward to obtain. However, stochastic differential equations might not always be an appropriate model, particularly if the change in an integer state variable is very small. For example, a stochastic differential equation for the change in a integer state variable represents a normal approximation to a Poisson random variable if the change in the state variable is sufficiently large at each time step and its mean and variance are equal (Gillespie 2009). If the change in state variable is small enough such that the normal approximation is no longer valid, then an alternative stochastic modeling approach could be used, such as a continuous-time Markov chain, to obtain analytical expressions for summary statistics, e.g., (Brett et al. 2017).

In conclusion, patterns in autocorrelation, coefficient of variation and power spectrum are robust to the form of stochasticity prior to system collapse. However, variance behavior prior to bifurcations may not follow any particular rules of thumb, but rather, be model or process-specific. We recommend that scientists and modelers carefully account for sources of noise when building models for systems on the verge of a tipping point. For example, at the scale of a laboratory microcosm experiment, it may be possible to write down a mechanistic model accounting for various sources of noise. We recommend developing alternative mechanistic models, using the models to obtain predictions for leading indicators, and then testing their predictions experimentally when possible. There are extensively documented ways of obtaining indicators from simulations [e.g., (Dakos et al. 2012; Kéfi et al. 2014)] and various toolboxes specific to early warning systems are available [e.g.,(Dakos et al. 2012; Boettiger and Hastings 2012; Ives and Dakos 2012)]. Nonetheless, our results support the baseline prediction

of increasing variance prior to a critical transition. We expect that prediction to hold if it is reasonable to assume that noise is external and affects a system as a whole, or if there is no clear description of how noise affects specific processes in a large-scale system.

Acknowledgements Much of this work was conducted while SMO was a Postdoctoral Fellow and DLB was a Graduate Research Assistant at the National Institute for Mathematical and Biological Synthesis, an Institute sponsored by the National Science Foundation through NSF Award # DBI-1300426, with additional support from The University of Tennessee, Knoxville. Additional support was obtained from North Carolina A&T State University. The authors would like to thank John Drake, Eamon O'Dea, Suzanne Lenhart and an anonymous reviewer for thoughtful comments on the manuscript.

Appendix A: Variance Approaches Zero from the Right

Since $v(r)$ is always positive, by definition $\lim_{r\to 0^+} v(r) = 0$ if and only if for all $\varepsilon > 0$ there exists some $\delta > 0$ so that $\frac{g(x^s,r)^2}{2|f'(x^s,r)|} < \varepsilon$ for each $r \in (0, \delta)$. This can be restated as: $\lim_{r\to 0^+} v(r) = 0$ if and only if for all $\varepsilon > 0$ there is $\delta > 0$ so that for each $r \in (0, \delta)$ we have

$$g(x^s, r)^2 < 2\varepsilon |f'(x^s, r)|. \tag{19}$$

Consequently, if inequality (19) holds in some neighborhood of the bifurcation point for every $\varepsilon > 0$, then the variance will approach 0 as r approaches the bifurcation point. Since we already have (10), inequality (19) implies that $\lim_{r\to 0^+} g(x^s, r)^2 = 0$ and that $g(x^s, r)^2$ approaches 0 more rapidly than $2|f'(x^s, r)|$. When (10) holds, both of these conditions on g are necessary conditions for $\lim_{r\to 0^+} v(r) = 0$, but inequality (19) is both necessary and sufficient. Comparing Fig. 2 with Table 6, we see that for models with intrinsic noise, the O–U variance curve declines to zero faster than the resilience term, and in each of these cases $\lim_{r\to 0^+} v(r) = 0$. The other case where $\lim_{r\to 0^+} v(r) = 0$ is with mechanistic environmental noise for the transcritical bifurcation case, where the O–U variance term also approaches zero more rapidly than the resilience term.

References

Allen EJ (2007) Modeling with Itô stochastic differential equations. Springer, Dordrecht

Allen LJS (2003) An introduction to stochastic processes with applications to biology. Prentice Hall, Upper Saddle River

Arnold L (1998) Random dynamical systems. Springer, Berlin

Bauch CT, Sigdel R, Pharaon J, Anand M (2016) Early warning signals of regime shifts in coupled human–environment systems. Proc Natl Acad Sci USA 113(51):14560–14567

Boerlijst MC, Oudman T, de Roos AM (2013) Catastrophic collapse can occur without early warning: examples of silent catastrophes in structured ecological models. PLoS ONE 8(4):e62033. https://doi.org/10.1371/journal.pone.0062033

Boettiger C, Hastings A (2012) Quantifying limits to detection of early warning for critical transitions. J R Soc Interface 9(75):2527–2539. https://doi.org/10.1098/rsif.2012.0125

Brett TS, Drake JM, Rohani P (2017) Anticipating the emergence of infectious diseases. J R Soc Interface 14(132):20170115
Carpenter SR, Brock WA (2006) Rising variance: a leading indicator of ecological transition. Ecol Lett 9(3):311–318
Carpenter SR, Ludwig D, Brock WA (1999) Management of eutrophication for lakes subject to potentially irreversible change. Ecol Appl 9(3):751. https://doi.org/10.2307/2641327
Dai L, Korolev KS, Gore J (2013) Slower recovery in space before collapse of connected populations. Nature 496(7445):355–8. https://doi.org/10.1038/nature12071
Dakos V, van Nes EH, D'Odorico P, Scheffer M (2012a) Robustness of variance and autocorrelation as indicators of critical slowing down. Ecology 93:264–271
Dakos V, Carpenter SR, Brock WA, Ellison AM, Guttal V, Ives AR, Kefi S, Livina V, Seekell DA, van Nes EH, Scheffer M (2012b) Methods for detecting early warnings of critical transitions in time series illustrated using simulated ecological data. PLoS One 7:e41010. https://doi.org/10.1371/journal.pone.0041010
Dakos V, van Nes EH, Scheffer M (2013) Flickering as an early warning signal. Theor Ecol 6(3):309–317. https://doi.org/10.1007/s12080-013-0186-4
Ditlevsen PD, Johnsen SJ (2010) Tipping points: early warning and wishful thinking. Geophys Res Lett. https://doi.org/10.1029/2010GL044486
Drake JM, Hay SI (2017) Monitoring the path to the elimination of infectious diseases. Trop Med Infect Dis 2(3):20
Fenichel N (1979) Geometric singular perturbation theory for ordinary differential equations. J Differ Equ 31:53–98
Gardiner CW (2004) Handbook of stochastic methods for physics, chemistry and the natural sciences. Springer, Berlin
Gillespie DT (2009) Deterministic limit of stochastic chemical kinetics. J Phys Chem B 113(6):1640–4. https://doi.org/10.1021/jp806431b
Guckenheimer J, Holmes P (1983) Nonlinear oscillations, dynamical systems, and bifurcations of vector fields, applied mathematical sciences, vol 42. Springer, New York
Han BA, Drake JM (2016) Future directions in analytics for infectious disease intelligence. EMBO Rep 17(6):785–789
Holling CS (1996) Engineering resilience versus ecological resilience. In: Schulze PC (ed) Engineering within ecological constraints. National Academy of Sciences, Washington, pp 31–44. https://doi.org/10.17226/4919. arXiv:1011.1669v3
Ives AR, Dakos V (2012) Detecting dynamical changes in nonlinear time series using locally linear state-space models. Ecosphere. https://doi.org/10.1890/ES11-00347.1
Ives AR, Dennis B, Cottingham KL, Carpenter SR (2003) Estimating community stability and ecological interactions from time series data. Ecol Monogr 73(2):301–330. https://doi.org/10.1890/0012-9615(2003)073[0301:ECSAEI]2.0.CO;2
Karesh WB, Dobson A, Lloyd-Smith JO, Lubroth J, Ma D, Bennett M, Aldrich S, Harrington T, Formenty P, Loh EH, Machalaba CC, Thomas MJ, Heymann DL (2012) Ecology of zoonoses: natural and unnatural histories. Lancet 380(9857):1936–45
Keeling M, Grenfell B (1999) Stochastic dynamics and a power law for measles variability. Philos Trans R Soc B Biol Sci 354(1384):769–776. https://doi.org/10.1098/rstb.1999.0429
Keeling MJ (2000) Simple stochastic models and their power-law type behaviour. Theor Popul Biol 58(1):21–31. https://doi.org/10.1006/tpbi.2000.1475
Keeling MJ, Rohani P (2008) Modeling infectious diseases in humans and animals. Princeton University Press, Princeton
Kéfi S, Guttal V, Brock WA, Carpenter SR, Ellison AM, Livina VN, Seekell DA, Scheffer M, van Nes EH, Dakos V (2014) Early warning signals of ecological transitions: methods for spatial patterns. PloS ONE 9(3):e92097. https://doi.org/10.1371/journal.pone.0092097
Kuehn C (2011) A mathematical framework for critical transitions: bifurcations, fast-slow systems and stochastic dynamics. Physica D 240:1020–1035
Lade SJ, Gross T (2012) Early warning signals for critical transitions: a generalized modeling approach. PLoS Comput Biol 8(2):e1002360. https://doi.org/10.1371/journal.pcbi.1002360
Lenton TM (2011) Early warning of climate tipping points. Nat Clim Change 1:201–209
Lenton TM, Held H, Kriegler E, Hall JW, Lucht W, Rahmstorf S, Schellnhuber HJ (2008) Tipping elements in the Earth's climate system. Proc Natl Acad Sci USA 105(6):1786–93

Lever JJ, van Nes EH, Scheffer M, Bascompte J (2014) The sudden collapse of pollinator communities. Ecol Lett 17(3):350–359

Ludwig D, Jones DD, Holling CS (1978) Qualitative analysis of insect outbreak systems: the spruce budworm and forest. J Anim Ecol 47(1):315–332. https://doi.org/10.2307/3939

Meiss JD (2007) Differential dynamical systems. Society for Industrial and Applied Mathematics, Philadelphia

Melbourne BA, Hastings A (2008) Extinction risk depends strongly on factors contributing to stochasticity. Nature 454(7200):100–103. https://doi.org/10.1038/nature06922

Nicolis C, Nicolis G (2014) Dynamical responses to time-dependent control parameters in the presence of noise: a normal form approach. Phys Rev E 89(2):022903. https://doi.org/10.1103/PhysRevE.89.022903

Nisbet RM, Gurney WSC (1982) Modelling fluctuating populations. Wiley, New York

O'Regan SM, Drake JM (2013) Theory of early warning signals of disease emergence and leading indicators of elimination. Theor Ecol 6(3):333–357. https://doi.org/10.1007/s12080-013-0185-5

O'Regan SM, Lillie JW, Drake JM (2016) Leading indicators of mosquito-borne disease elimination. Theor Ecol 9(3):269–286. https://doi.org/10.1007/s12080-015-0285-5

Pimm SL (1984) The complexity and stability of ecosystems. Nature 307:321–326. https://doi.org/10.1038/315635c0. arXiv:1011.1669v3

Quail T, Shrier A, Glass L (2015) Predicting the onset of period-doubling bifurcations in noisy cardiac systems. Proc Natl Acad Sci USA 112(30):9358–63. https://doi.org/10.1073/pnas.1424320112

Scheffer M (2009) Critical transitions in nature and society. Princeton University Press, Princeton

Scheffer M, Hosper SH, Meijer M-L, Moss B, Jeppesen E (1993) Alternative equilibria in shallow lakes. Trends Ecol Evolut 8(8):275–279

Scheffer M, Bascompte J, Brock WA, Brovkin V, Carpenter SR, Dakos V, Held H, van Nes EH, Rietkerk M, Sugihara G (2009) Early warning signals for critical transitions. Nature 461:53–59

Scheffer M, Carpenter SR, Lenton TM, Bascompte J, Brock W, Dakos V, van de Koppel J, van de Leemput IA, Levin SA, van Nes EH, Pascual M, Vandermeer J (2012) Anticipating critical transitions. Science 338:344–348

Sharma Y, Abbott KC, Dutta PS, Gupta AK (2014) Stochasticity and bistability in insect outbreak dynamics. Theor Ecol 8(2):163–174. https://doi.org/10.1007/s12080-014-0241-9

Strogatz SH (1994) Nonlinear dynamics and chaos with applications to physics, biology chemistry and engineering. Addison-Wesley, Reading

Trefois C, Antony PM, Goncalves J, Skupin A, Balling R (2015) Critical transitions in chronic disease: transferring concepts from ecology to systems medicine. Curr Opin Biotechnol 34:48–55. https://doi.org/10.1016/j.copbio.2014.11.020

van Nes EH, Scheffer M (2007) Slow recovery from perturbations as a generic indicator of a nearby catastrophic shift. Am Nat 169(6):738–747. https://doi.org/10.1086/516845

Veraart AJ, Faassen EJ, Dakos V, van Nes EH, Lürling M, Scheffer M (2012) Recovery rates reflect distance to a tipping point in a living system. Nature 481(7381):357–359. https://doi.org/10.1038/nature10723

Wang R, Ja D, Langdon PG, Zhang E, Yang X, Dakos V, Scheffer M (2012) Flickering gives early warning signals of a critical transition to a eutrophic lake state. Nature 492(7429):419–22. https://doi.org/10.1038/nature11655

Wissel C (1984) A universal law of the characteristic return time near thresholds. Oecologia 65(1):101–107. https://doi.org/10.1007/BF00384470